JREE: Vol. 7, No. 2, (Spring 2020) 52-63

Journal of Renewable Energy and Environment

Journal Homepage: www.jree.ir

Research Article

A Novel Local Control Technique for Converter-Based Renewable Energy Resources in the Stand-Alone DC Micro-Grids

Arash Abedi, Behrooz Rezaie*, Alireza Khosravi, Majid Shahabi

Department of Control, Faculty of Electrical and Computer Engineering, Babol Noshirvani University of Technology, Babol, Iran.

PAPER INFO

Paper history:
Received 12 February 2020
Accepted in revised form 12 May 2020

Keywords:
DC/DC Converter
Stability Analysis
Stand-Alone DC Micro-Grid
Switching Function

ABSTRACT

This paper presents a novel local control method for the converter-based renewable energy resources in a stand-alone DC micro-grid based on energy analysis. The studied DC micro-grid comprises the renewable energy resources, back-up generation unit, and battery-based energy storage system, which are connected to the common DC-bus through the buck and bidirectional buck-boost converters. The proposed control method satisfies the stability of the micro-grid output variables, along with current control and voltage regulation by controlling the switching functions of the converters, regardless of the energy resource dynamics. The dynamic component of the switching function is extracted as a control signal using the state-feedback through a mathematical method. The control inputs are designed based on Lyapunov stability theorem to guarantee the stability of output variables (DC-bus voltage and generated currents) in a stand-alone DC micro-grid through an energy analysis. The proposed distributed controller can be easily generalized as a platform with all kinds of the stand-alone DC micro-grids comprising any type or number of distributed generations such as renewable energy resources, fossil-fuel-based generations, and energy storage units. Other features of this local control method are simplicity, celerity, comprehensiveness, and independence of the distributed generations. The dynamic performance assessment of the proposed controller is verified through a simulation in MATLAB/SIMULINK® environment. The results validate the accuracy and stability of the proposed control strategy in various operating conditions.

1. INTRODUCTION

Recently the global efforts to reduce the use of fossil fuels, growing energy demand, increased number of renewable energy resources (RERs) [1] and more important advancements in power electronics have led to the modernization of the existing power system [2]. Introduction of AC and DC micro-grids including distributed generations (DGs) such as RERs, energy storage systems (ESS), gas-micro-turbine generators, etc. made it possible for engineers to reshape the conventional power system [3].

The micro-grids are emerging in the modern power system and becoming an attractive choice due to the integration of DGs such as photovoltaics, wind-turbines, storage devices, and controllable loads, which can operate in either isolated or grid-connected mode. However, the issue of reliability and stability has not been accomplished yet within these small-scale distribution grids [4]. In a grid-connected AC micro-grid, the main grid standards for frequency and voltage are utilized, and energy stability is important for power quality [5]. However, in the stand-alone operation mode, the frequency and the voltage must be stabilized and regulated via a control system [6-8].

In a stand-alone micro-grid supplying a residential area, most of the consumptions are DC loads, such as electronic, telecommunication and audio-visual devices. Moreover, the other loads can be supplied either by AC or DC such as air-conditioning or lighting devices [9]. In fact, distributing energy in DC form is in favor of distribution suppliers due to the reduced number of converters, limited frequency control challenges, higher efficiency, and minimized costs. Thus, DC micro-grids is a proper choice for providing remote residential areas. Still, in such networks, the voltage regulation, voltage stabilization, and energy management are vital to improve the power quality and provide a reliable and efficient power [10, 11]. Therefore, proposing comprehensive methods for controlling and stability of the stand-alone DC micro-grids is of great importance.

Some studies in the literature have been devoted to the DC voltage control strategies and energy management control systems. In [12], the authors employed a three-level control strategy to stabilize the DC-bus voltage in various operation conditions (i.e. load change, generation fluctuations) in a DC micro-grid with variable sources and loads. In this study, a control program based on PI and droop controllers has been presented. However, the stability has not been guaranteed. Augustine et al. [13] developed an adaptive droop control technique to manage the current sharing and voltage regulation in a low voltage DC micro-grid. There are three points to note about this reference. First, in this study, the researchers have not addressed the issues of micro-grid stability. Besides, only two DGs with the same type of converter have been studied. Finally, the authors have neglected the role of energy storage units which is vital in the stand-alone micro-grids with RERs, because the challenges of bidirectional power flow are crucial in energy analysis and stability studies. Dizqah et al. [14] proposed a control strategy based on model predictive control (MPC) to manage the voltage stability and energy flow between wind, solar and battery devices, as well as battery management in a DC micro-grid. Anand et al. [15] presented a decentralized droop

*Corresponding Author's Email: brezaie@nit.ac.ir (B. Rezaie)

controller by applying a low bandwidth communication to the conventional droop controllers, to improve voltage regulation in an isolated DC micro-grid. However, the dynamic behavior of controllers via a detailed model of the converter has not been considered in [14,15], while, in stand-alone micro-grids, the dynamic behavior of the converters considerably influences the voltage quality in small-signal and should be considered in the controller's design [16].

In [17] a droop control strategy has been proposed for voltage regulation in an islanded DC micro-grid based on energy stability analysis. However, the DGs in the DC micro-grid modeled simply as the ideal constant DC voltage sources equalized with transmission impedance. This simplification is presumed for nonlinear stability analysis and prediction of the qualitative behavior of the system as a function of model parameters. Moreover, the dynamic characteristics of the converters have been neglected in the model. Herrera et al. [18] considered the loads in the DC micro-grid as constant power loads due to high switching frequency, while the local stability analysis and controller design presented using the Lyapunov function. Liu et al. [19] represented small-signal modeling of an islanded DC micro-grid including a synchronous generator as the generation source of the micro-grid and an induction motor as the micro-grid load. In their developed model, the dynamic effects of the constant power load, and the filter design parameters on system stability, have been evaluated. However, the current and voltage control in the micro-grid have been performed exclusively via a synchronous generator connected to a rectifier, and the dynamic role of the power converters has been neglected.

In [20], a kind of linear mathematical modeling represented for state-space of all the converters in a DC micro-grid considering the currents, voltages and droop controllers, likewise, the dynamic stability analysis of the system and controllers has been performed. Furthermore, modeling the buck converters in [20] performed using the average model, where the duty-cycle of the converters was adjusted using the simple conventional PI controllers.

In [21] the authors employed the Lyapunov theorem for stabilization and optimized operation assessment in a stand-alone DC micro-grid using a nonlinear model, where the resources are battery storage devices. In this study, the two battery branches represent a fast charging branch and a slower charging one. The duty-cycles of the converters connected to the batteries have been controlled via a constant gain PI controller through a droop control method. Furthermore, a reduced-order model for DC/DC converters has been used that their performance differs from that of real samples and this issue affects the stability analysis. Although in [20,21], the researchers have considered stability, the PI controller as a linear operator could not provide acceptable accuracy in the range of the actual non-linear performance [22].

The topics related to stand-alone DC micro-grids have been the focus of research just in the last decade [23]. Hence, a lot of issues have remained intact or rarely focused on the simultaneous study on local control and stability analysis about the precise concept "stand-alone DC micro-grids", For instance, some studies have been privatized on specified energy resources models and the proposed control approaches have not been presented comprehensively for all kinds of resources [13,19,24]. Some studies have proposed model-independent approaches, but they have tested their proposed method on the resources with inherently stable dynamics such as constant DC supply, battery, or PV and the validity of these methods has not considered for rotational electro-mechanical dynamics such as wind turbines, gas-micro-turbines and the like [17,21,25]. A lot of researches has simplified the modeling of micro-grids or converters or have used linear controllers to control a nonlinear system. These issues challenge the effectiveness of these methods in terms of actual performance, faced with nonlinearities, uncertainties, and disturbances [12,15,17,19-21]. In centralized control schemes, the control structure is reconstructed and updated to plug in additional resources. Moreover, the error in the central controller causes all units to malfunction. Besides, there is a pressing need for information and communication technologies [26,27]. Even in some distributed control schemes, despite the plug-and-play capability, there is complex bidirectional communication between the local controllers [28]. These issues increase the costs of establishing, maintaining, and reduce micro-grid reliability.

On the other hand, the converter is one of the controllable devices [23] that could potentially control and stabilize the output variables of the micro-grid as a general local platform regardless of the resource dynamics. In this case, the switching function of the converter could be considered as a non-physical control command. In addition to the challenges discussed above, in [29-32] and all the above-mentioned references, the effects of switching functions have not been examined on the dynamic behavior of converters.

In order to cover a significant portion of the recent challenges, the main objectives of our research are: (1) designing a generalized distributed local controller for RERs and any type of converter-based resources in stand-alone DC micro-grids; and (2) stabilizing the output voltage and currents of the stand-alone DC micro-grid through simply controlling the switching function of the converters regardless of resource dynamics.

The hypothesis of our study is so comprehensive that it covers various kinds of stand-alone DC micro-grids as follows:

- The stand-alone DC micro-grid consists of *n* resources.
- A battery unit represents all the ESSs in the micro-grid.
- The resources and the loads are connected to the common DC bus.
- All resources are connected to the bus via full-order DC/DC converters. (buck converter for DGs and bidirectional buck-boost converter for battery unit).

This paper represents a novel control strategy based on the direct Lyapunov method (DLM) to perform current and DC-bus voltage regulation considering the switching function control. In fact, the DC-bus voltage regulation is implemented via decreasing the effects of the energy oscillations. This approach determined a detailed and full-order dynamic model for the steady-state and dynamic operation of the converters connected to the DGs and the battery energy storage system (BESS). In fact, the proposed controller performs the voltage stabilizing by reducing the volatility of the generated currents. This is done by controlling the switching functions of the DC/DC converters. In this control plan, the steady-state and dynamic parts of the switching functions were calculated separately through a mathematical definition for variables errors. Then, the dynamic component of the switching function is computed using DLM in such a way the errors of the state-variables which are due to the system fluctuations are always damped. This simple and agile dynamic calculation acts as a closed-loop stabilizer-regulator controller.

The prominent features of this approach are its rapid and simple execution, fast transient-state response, low range dynamic oscillation, and its ability to generalize with all the stand-alone micro-grids comprising any type or number of RERs, ESSs, and the other DGs. Moreover, as can be seen in Figure 1, the controllers of the converters connected to the DGs are independent of each other and the only communication is conducted into the controller of the converter connected to the BESS. This feature facilitates the installation of new DGs in development plans.

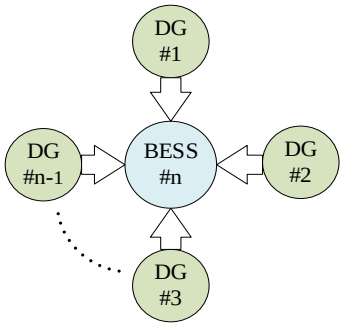

Figure 1. The communication topology of the proposed local controllers.

In summary, the main novelties and contributions of this work are as follows:

- The dynamic component of the switching function of the converters is extracted, regardless of resource dynamics, using the state-feedback through a mathematical method.
- This switching function is utilized as the control signal to stabilize the output voltage and currents of the stand-alone DC micro-grid.
- A generalized distributed local controller is proposed by presenting and proving a novel comprehensive stability theorem.
- This novel controller is applicable to all kinds and any number of converter-based energy resources in a stand-alone DC micro-grid.

The rest of this paper is organized as follows: In section 2, the precise model of the system is introduced. The methodological approach is explained through the steady-state analysis in section 3 and in section 4 through the energy analysis of the system by applying the DLM, the proper controller architecture is represented. Section 5 is devoted to the simulation of a stand-alone DC micro-grid consists of three DGs and a BESS controlled by the proposed controller, and evaluating two scenarios based on this system and the simulation results using MATLAB/SIMULINK® are discussed. The conclusion is drawn in the last section.

2. MULTI-SOURCE DC MICRO-GRID STRUCTURE

The general scheme of the proposed stand-alone DC micro-grid has been shown in Figure 2. This structure consists of n units, supplying the load so that, n-1 units are the DG units such as RERs or other energy resources connected to the BCs, and one unit is the BESS consists of a lithium-battery connected to a BBC. However, the proposed local control method is independent of the resource model. The BESS unit is employed to provide a constant DC-bus voltage with acceptable precision and agility for the stand-alone DC micro-grid in the steady-state operation or under dynamic changes due to the load change. In this section, the detailed dynamic model of the converters is described.

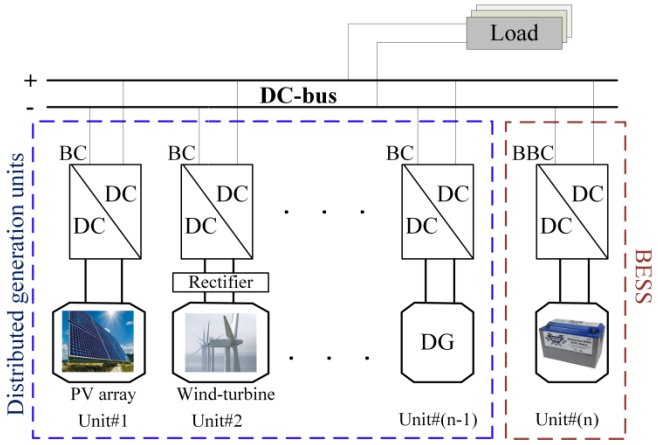

Figure 2. A typical stand-alone DC micro-grid configuration.

Considering the high initial cost of battery purchase, as well as the limited lifetime of the batteries with finite charging/discharging cycles, the BESS unit in this system is controlled only to regulate the DC-bus voltage, rather than supplying as an alternative resource. The controllers designed in this paper as the main contribution of this work are as follows:

- The controllers for the BCs connected to the DGs, to regulate the needed currents.
- A controller for the BBC connected to the BESS unit to regulate the desired DC voltage.

2.1. Buck DC/DC converters

As shown in Figure 3, the basic function of the BC is the current of an inductor controlled by switches. Therefore, the output current of the converter can be controlled by controlling the switching function. The switch (usually can be a power transistor) and diode have zero voltage drop and zero current in OFF and ON mode respectively. Input and output capacitors are considered respectively for smoothing the input and output currents of the BC. Since the injected power from the DGs to the DC micro-grid is accomplished by the BCs, a complete dynamic description of these converters is required. As shown in Figure 3, the dynamical scheme of a typical BC can be modeled as:

$$\begin{cases} \dfrac{dv_{ij}}{dt} = \dfrac{i_{ij}}{C_{ij}} - \dfrac{i_{Lj}u_j}{C_{ij}} \\ \dfrac{di_{Lj}}{dt} = \dfrac{v_{ij}u_j}{L_j} - \dfrac{v_{bus}}{L_j} \\ \dfrac{dv_{bus}}{dt} = \dfrac{i_{Lj}}{C_{oj}} - \dfrac{i_{oj}}{C_{oj}} \end{cases} \quad , \quad j = 1,2,3 \qquad (1)$$

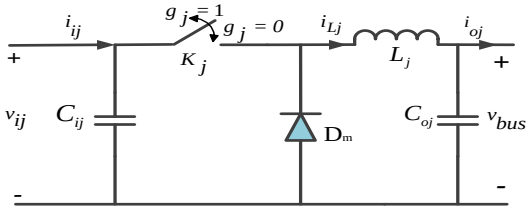

Figure 3. The detailed structure of a typical BC.

where C_{ij}, C_{oj}, L_j are respectively the input capacitor, output capacitor and the inductance of the BC, u_j, g_j, v_{ij} and i_{ij} are respectively the switching function, switching signal, input voltage and the input current of the BC. Moreover, i_{Lj} is the inductance current, v_{bus} the output voltage equals to the DC-bus voltage, and i_{oj} the output current of the BC that represents the contribution of each DG in the stand-alone DC micro-grid. In Equation (1), j represents the number of each of the DGs. K_j, represents an electrical switch that can be any kind of the typical controllable electrical switches. The switching signals (g_j) are generated by applying the switching function (u_j) to the Pulse Width Modulation (PWM), in the manner as shown in Figure 4. Finally, as shown in Figure 3, the signals g_j indicate the switches K_j be ON or OFF [33].

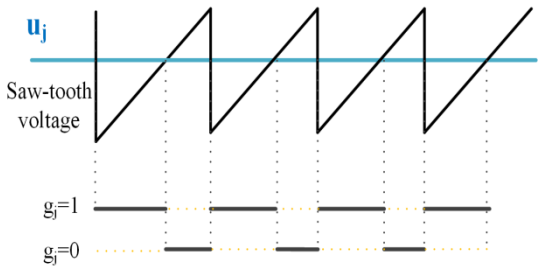

Figure 4. Switching signal generating by PWM.

2.2. Buck-boost DC/DC converter

The bidirectional BBC is the best choice for the operation of charging and discharging in a BESS unit. In Figure 5, a typical bidirectional BBC has been designed, and Equation (2) defines the function of the BBC in terms of the switching condition:

$$\begin{cases} \dfrac{di_{Ln}}{dt} = \dfrac{v_{in}}{L_n} - \dfrac{u_n v_{bus}}{L_n} \\ \dfrac{dv_{bus}}{dt} = \dfrac{u_n i_{Ln}}{C_{on}} - \dfrac{i_{on}}{C_{on}} \end{cases} \quad (2)$$

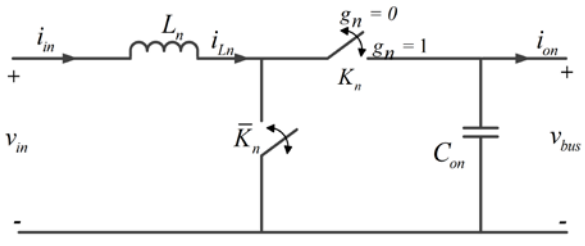

Figure 5. The detailed structure of a typical BBC.

where C_{on}, L_n, g_n and u_n are respectively the output capacitor, inductance, switching signal and the switching function of the BBC. Moreover, $i_{Ln} = i_{in}$ and v_{in} is respectively the input current and input voltage of the BBC, v_{bus} and i_{on} represents the output current of the BBC and the DC-bus voltage. In fact, the current i_{on} represents the contribution of the BESS in the DC micro-grid. During the discharge mode, $\bar{K}_n$ is open and the switching operation is performed on K_n. On the contrary, during the recharge mode, K_n is closed and the switching operation is performed on $\bar{K}_n$, also in this case, ($\bar{u}_n = 1 - u_n$) replaced by u_n in the Equation (2). The dynamic Equation (1) and (2) are used for the aim of regulating the current and voltage of the DC-bus in the stand-alone DC micro-grid.

The overall scheme in this study concentrates on the dynamic part of the DC/DC converters. All fluctuations and disturbances caused by the mechanical and electrical parts of various kinds of the DGs will ultimately affect the input voltages and currents of the converters, and these effects have been examined in this study. However, the proposed design in this paper can be expanded to an implemental scheme, since different secondary controllers can be employed to control and manage various energy resources in the stand-alone DC micro-grids.

3. STEADY-STATE ANALYSIS

To control the DC-bus voltage in the steady-state operation, the switching functions of all BCs and BBC in the Equation (1) and (2) should be achieved by substituting the desired values of all state variables, marked by '*' superscripts. According to Figure 3, considering the switching functions as a control signal, and through solving the Equation (1) and (2), the averaged switching functions u_j^* are obtained as follows:

$$u_j^* = \frac{i_{ij}^* - C_{ij}\dot{v}_{ij}^*}{2i_{Lj}^*} + \frac{L_j\dot{i}_{Lj}^* + v_{bus}^*}{2v_{ij}^*} \quad , \quad j = 1, 2, 3, \ldots, (n-1) \quad (3)$$

$$u_n^* = \frac{v_{in}^* - L_n\dot{i}_{Ln}^*}{2v_{bus}^*} + \frac{C_{on}\dot{v}_{bus}^* + i_{on}^*}{2i_{Ln}^*} \quad (4)$$

As can be seen, all the state variables are considered to achieve the averaged switching functions. Obviously, in this study to achieve the voltage stability and current regulation, the values of desired voltages and currents $v_{ij}^*, i_{Lj}^*, i_{Ln}^*, v_{bus}^*, i_{ij}^*$ are constant. Therefore, the steady-state references $\dot{v}_{ij}^*, \dot{i}_{Lj}^*, \dot{i}_{Ln}^*, \dot{v}_{bus}^*$ are zero. Hence, according to Figure 3, where $\dot{v}_{bus}^*$ is considered zero, the desired value of i_{Lj}^* represents i_{oj}^*. Consequently, the simplified results of the Equation (3) and (4) are respectively equal to $\frac{i_{ij}^*}{2i_{Lj}^*} + \frac{v_{bus}^*}{2v_{ij}^*}$ and $\frac{v_{in}^*}{2v_{bus}^*} + \frac{i_{on}^*}{2i_{Ln}^*}$. These desired reference values are used for calculating the deviations of the variables from their desired steady-state values. For this purpose, v_{ij}^* and v_{bus}^* are respectively considered equal to the nominal voltages of the DGs, and the nominal voltage of the DC-bus. The output currents i_{oj}^* and i_{on}^* are issued by the outer layer controllers based on different methods of energy management and power-sharing in the micro-grids. Consequently, the input currents i_{ij}^* and i_{Ln}^* can be calculated based on the equality of input/output power of the converters. To stabilize the DC-bus voltage, in this scheme, i_{on}^* is determined based on the difference between the generated and needed currents. Further details are provided in section 4.2.2.

4. ENERGY ANALYSIS AND DLM-BASED CONTROLLER DESIGN

The DLM analysis has been used to stabilize all the state variables in the proposed DC micro-grid, to reach their equilibrium points in a way that the micro-grid has a stable operation in steady and transient states. This method is based on the energy analysis of the state variables of the system [34].

4.1. Energy equations

First, the vectors of the state variables and their desired values are respectively defined as (5), (6):

$$\mathbf{X} = \begin{bmatrix} \mathbf{v_i} & \mathbf{i_L} & i_{Ln} & v_{bus} \end{bmatrix}^T \tag{5}$$

$$\mathbf{X} = \begin{bmatrix} \mathbf{v_i^*} & \mathbf{i_L^*} & i_{Ln}^* & v_{bus}^* \end{bmatrix}^T \tag{6}$$

where $\mathbf{X}$ and $\mathbf{X}^*$ represent the vectors of the state variables of all converters and their desired values, $(\mathbf{v_i}, \mathbf{i_L})$, $(\mathbf{v_i^*}, \mathbf{i_L^*})$ are respectively the vectors of the state variables of the BCs and their desired values, as described below:

$$\mathbf{v_i} = \begin{bmatrix} v_{i1} & v_{i2} & \cdots & v_{i(n-1)} \end{bmatrix} \tag{7}$$

$$\mathbf{v_i^*} = \begin{bmatrix} v_{i1}^* & v_{i2}^* & \cdots & v_{i(n-1)}^* \end{bmatrix} \tag{8}$$

$$\mathbf{i_L} = \begin{bmatrix} i_{L1} & i_{L2} & \cdots & i_{L(n-1)} \end{bmatrix} \tag{9}$$

$$\mathbf{i_L^*} = \begin{bmatrix} i_{L1}^* & i_{L2}^* & \cdots & i_{L(n-1)}^* \end{bmatrix} \tag{10}$$

So, the vector of the state variables errors can be written as:

$$\mathbf{E} = \mathbf{X} - \mathbf{X}^* = \begin{bmatrix} \mathbf{e_{v_i}} & \mathbf{e_{i_L}} & e_{i_{Ln}} & e_{v_{bus}} \end{bmatrix}^T \tag{11}$$

where $\mathbf{e_{v_i}} = \mathbf{v_i} - \mathbf{v_i^*}$, $\mathbf{e_{i_L}} = \mathbf{i_L} - \mathbf{i_L^*}$, $e_{i_{Ln}} = i_{Ln} - i_{Ln}^*$, $e_{v_{bus}} = v_{bus} - v_{bus}^*$. In this way, the exact energy equation related to the errors of the state variables can be considered as the Lyapunov function, so that:

$$W_e(x) = \frac{1}{2} \mathrm{tr}[\mathrm{diag}(\mathbf{B}).\mathrm{diag}(\mathbf{E})^2] \tag{12}$$

where, based on (1) and (2), and assuming the output filter capacitors $C_{o1} = C_{o2} = C_{o3} = \ldots = C_{on} = C_o$, the vector $\mathbf{B}$ and its arrays in (12) are extracted as follows:

$$\mathbf{B} = \begin{bmatrix} \mathbf{C_i} & \mathbf{L} & L_n & nC_o \end{bmatrix}^T \tag{13}$$

$$\mathbf{C_i} = \begin{bmatrix} C_{i1} & C_{i2} & \cdots & C_{i(n-1)} \end{bmatrix} \tag{14}$$

$$\mathbf{L} = \begin{bmatrix} L_1 & L_2 & \cdots & L_{(n-1)} \end{bmatrix} \tag{15}$$

Subsequently, the derivative of the energy equation (12) is calculated as (16):

$$\dot{W}_e(x) = \mathrm{tr}[\mathrm{diag}(\mathbf{B}).\mathrm{diag}(\mathbf{E}).\mathrm{diag}(\dot{\mathbf{E}})] \tag{16}$$

By applying (11) and (13)-(15) to Equation (16) and after sorting out, all terms of (16) can be achieved as:

$$\dot{W}_e(x) = \sum_{j=1}^{n-1} C_{ij} e_{v_{ij}} \dot{e}_{v_{ij}} + \sum_{j=1}^{n-1} L_j e_{i_{Lj}} \dot{e}_{i_{Lj}} + L_n e_{i_{Ln}} \dot{e}_{i_{Ln}} + nC_o e_{v_{bus}} \dot{e}_{v_{bus}} \tag{17}$$

In (17), the first two terms refer to the DG units, which are connected to the BCs, and the other terms refer to the BESS unit connected through BBC.

4.2. DLM-based controller and stability analysis

To design a proper controller to regulate the generated currents of the DG units, and with the aim of stabilizing the DC-bus voltage through regulating the current of the BESS unit, the switching functions of the BCs and BBC are separated into two components u_j^* and U_j, such that:

$$u_j = u_j^* - U_j \quad , \quad j = 1, 2, \ldots, n \tag{18}$$

These components are respectively considered as the steady-state components and the dynamic components of the control signals. The steady-state components are the same as the averaged switching functions, have been defined previously in (3) and (4). In fact, U_j represents the dynamic effects of the state variables errors in each converter. Finally, the proper control signal is obtained by subtracting u_j^* and U_j. By applying (18) and (11) into (1) and (2), all terms of (17) can be rewritten as follows:

$$\sum_{j=1}^{n-1} C_{ij} e_{v_{ij}} \dot{e}_{v_{ij}} = \sum_{j=1}^{n-1} \underbrace{(i_{ij} - i_{ij}^*)}_{E_{i_{ij}}} e_{v_{ij}} - \underbrace{\sum_{j=1}^{n-1} u_j e_{i_{Lj}} e_{v_{ij}}}_{*} + \sum_{j=1}^{n-1} U_j i_{Lj}^* e_{v_{ij}} \tag{19}$$

$$\sum_{j=1}^{n-1} L_j e_{i_{Lj}} \dot{e}_{i_{Lj}} = \underbrace{\sum_{j=1}^{n-1} u_j e_{i_{Lj}} e_{v_{ij}}}_{*} - \sum_{j=1}^{n-1} U_j v_{ij}^* e_{i_{Lj}} - \underbrace{e_{v_{bus}} \sum_{j=1}^{n-1} e_{i_{Lj}}}_{**} \tag{20}$$

$$nC_o e_{v_{bus}} \dot{e}_{v_{bus}} = \underbrace{e_{v_{bus}} u_n e_{i_{Ln}}}_{***} - e_{v_{bus}} U_n i_{Ln}^* - e_{v_{bus}} \underbrace{\sum_{j=1}^{n} (i_{oj} - i_{oj}^*)}_{E_{i_{Load}}} + \underbrace{e_{v_{bus}} \sum_{j=1}^{n-1} e_{i_{Lj}}}_{**} \tag{21}$$

$$L_n e_{i_{Ln}} \dot{e}_{i_{Ln}} = \underbrace{(v_{in} - v_{in}^*)}_{E_{v_{in}}} e_{i_{Ln}} - \underbrace{e_{v_{bus}} u_n e_{i_{Ln}}}_{***} + v_{bus}^* U_n e_{i_{Ln}} \tag{22}$$

where $E_{i_{ij}}$ and $E_{v_{in}}$ are respectively the errors of the input currents of the BCs, and the error of the input voltage of the BBC connected to the BESS. Since, $i_{Load} = \sum_{j=1}^{n} i_{oj}$ and $i_{Load}^* = \sum_{j=1}^{n} i_{oj}^*$, therefore, $E_{i_{Load}}$ is the difference between the sum of the generated currents and their desired values, that it is equal to the difference between the injected currents and total load demand $(i_{Load} - i_{Load}^*)$. As can be seen, in the Equations (19)-(22), each pair of the terms identified by '*', '**' and '***', are respectively symmetric, so the final simplified equation by replacing (19)-(22) into (17), can be rewritten as:

$$\dot{W}_e(x) = \sum_{j=1}^{n-1} e_{v_{ij}} E_{i_{ij}} + \sum_{j=1}^{n-1} U_j (i^*_{Lj} e_{v_{ij}} - v^*_{ij} e_{i_{Lj}}) + U_n (v^*_{bus} e_{i_{Ln}} - i^*_{Ln} e_{v_{bus}}) + E_{v_{in}} e_{i_{Ln}} - e_{v_{bus}} E_{i_{Load}} \quad (23)$$

According to DLM, to reach the global asymptotical stability, if the total system energy is positive, therefore its derivative must be definitely negative [34]. On this basis, to calculate the dynamic part of the switching functions as a component of the control signal, we can state the following theorem:

Theorem 1. In a DC micro-grid with the energy equation of the state variables errors defined by (12), and the derivative of the energy equation defined by (23), there are $\left(U_j, j = 1, 2, ..., n\right)$ equal to (24) and (25) making the system globally asymptotically stable according to the Lyapunov definition, such that:

$$U_j = \frac{\alpha_j (i^*_{Lj} e_{v_{ij}} - v^*_{ij} e_{i_{Lj}})^2 - e_{v_{ij}} E_{i_{ij}}}{i^*_{Lj} e_{v_{ij}} - v^*_{ij} e_{i_{Lj}}}, \forall \alpha_j < 0, j = 1, 2, ..., (n-1) \quad (24)$$

$$U_n = \frac{\alpha_n (v^*_{bus} e_{i_{Ln}} - i^*_{Ln} e_{v_{bus}})^2 + e_{v_{bus}} E_{i_{Load}} - E_{v_{in}} e_{i_{Ln}}}{v^*_{bus} e_{i_{Ln}} - i^*_{Ln} e_{v_{bus}}}, \forall \alpha_n < 0 \quad (25)$$

Proof. At first, we consider the Lyapunov stability conditions [34]:

$$\begin{cases} W_e(0) = 0 \\ W_e(x) > 0, \quad \forall x \neq 0 \\ W_e(x) \to \infty, \quad \text{as} \quad \|x\| \to \infty \\ \dot{W}_e(x) < 0, \quad \forall x \neq 0 \end{cases} \quad (26)$$

According to (12), it is obvious that $W(0) = 0$, $W(x) > 0$ for all $x \neq 0$ and $W(x) \to \infty$ as $\|x\| \to \infty$. To establish all constraints of the Lyapunov stability theory, we assume that (23) is negative. A rigorous approach is that the energy equation of each unit is negative. This procedure helps to prove the stability of the micro-grid in the various situation of mono-source to multi-source generation, even regardless of the participation of the BESS unit. As a result, the distributed performance of the controllers is also guaranteed. In this approach, (23) can be divided into two general parts. One part contains the first two terms, referring to the DG units connected to the BCs, and the other part contains remained terms, referring to the BESS unit connected to the BBC, supposing both terms are negative. As described above, we have:

$$e_{v_{ij}} E_{i_{ij}} + U_j (i^*_{Lj} e_{v_{ij}} - v^*_{ij} e_{i_{Lj}}) < 0 \quad (27)$$

After replacing (24) into (27):

$$e_{v_{ij}} E_{i_{ij}} + \left(\frac{\alpha_j (i^*_{Lj} e_{v_{ij}} - v^*_{ij} e_{i_{Lj}})^2 - e_{v_{ij}} E_{i_{ij}}}{i^*_{Lj} e_{v_{ij}} - v^*_{ij} e_{i_{Lj}}} \right) \left(i^*_{Lj} e_{v_{ij}} - v^*_{ij} e_{i_{Lj}} \right) < 0 \quad (28)$$

$$\Rightarrow \alpha_j (i^*_{Lj} e_{v_{ij}} - v^*_{ij} e_{i_{Lj}})^2 < 0 \quad \Rightarrow \quad \alpha_j < 0 \quad (29)$$

Therefore, it is concluded that Equation (29) is always true for $\alpha_j < 0$. Similarly, for the other parts of (23), we assume:

$$U_n (v^*_{bus} e_{i_{Ln}} - i^*_{in} e_{v_{bus}}) + E_{v_{in}} e_{in} - e_{v_{bus}} E_{i_{Load}} < 0 \quad (30)$$

After replacing (25) into (30):

$$\left(\frac{\alpha_n (v^*_{bus} e_{i_{Ln}} - i^*_{in} e_{v_{bus}})^2 + e_{v_{bus}} E_{i_{Load}} - E_{v_{in}} e_{i_{Ln}}}{\left(v^*_{bus} e_{i_{Ln}} - i^*_{in} e_{v_{bus}} \right)} \right) \times \left(v^*_{bus} e_{i_{Ln}} - i^*_{in} e_{v_{bus}} \right) + E_{v_{in}} e_{i_{Ln}} - e_{v_{bus}} E_{i_{Load}} < 0 \quad (31)$$

$$\Rightarrow \quad \alpha_n (v^*_{bus} e_{i_{Ln}} - i^*_{Ln} e_{v_{bus}})^2 < 0 \quad \Rightarrow \quad \alpha_n < 0 \quad (32)$$

It is concluded that (32) is always true for $\alpha_n < 0$. Consequently, by applying (24) and (25), the derivative of the energy equation of the system will always be negative, therefore all conditions of the Lyapunov stability theory are satisfied, and the system is globally asymptotically stable according to the Lyapunov definition, so the theorem is proved.

After clearing the effects of the dynamic errors of the state variables from the average switching function u^*_j, the revised switching functions $u_j = u^*_j - U_j$ are applied to the PWM signal generator as a control command and consequently, the switching signals g_j are generated and applied to the converters.

4.2.1. Current regulating

As we can see in Equation (24), all errors of the state variables, input variables, and their desired values are involved in (24) that affect the output currents of the DGs. According to this equation, it is obvious that choosing the proper Lyapunov function leads to the accuracy and agility of the controller in eliminating the deviations. The signals $U_j, j = 1, 2, ..., (n-1)$ are the dynamic components of the BC switching functions and related to the deviations of the variables on output currents. The current control design is based on Equations (3), (18), and (24). According to Theorem 1, calculating $U_j, j = 1, 2, ..., (n-1)$ through Equation (24) will lead to system stability. Therefore, the controller calculates $U_j, j = 1, 2, ..., (n-1)$ at each step based on the state-feedback according to Figure 6. Since the switching function is placed in the energy equations equal to (18), by subtracting U_j from u^*_j, the modified switching functions are obtained dynamically and applied to the converter. The alpha presence of all the variables affecting the output currents in the equation. As a result, this increases the coefficients weigh the effects of the errors. Although for any negative values of α_j, the stability of the output currents and damping the oscillation are guaranteed, but the proper adjustment of α_j will reduce the steady-state error and increase the response rapidity as can be seen in section 5. According to Figure 6, the BC controller calculates u^*_j and U_j based on the desired reference current $i^*_{oj}, j = 1, 2, ..., (n-1)$ and applies the modified switching signal u_j as a control signal to the PWM subsequently. Finally, based on Figure 4, the proper switching signals are generated and applied to the BC as described in section 2.1.

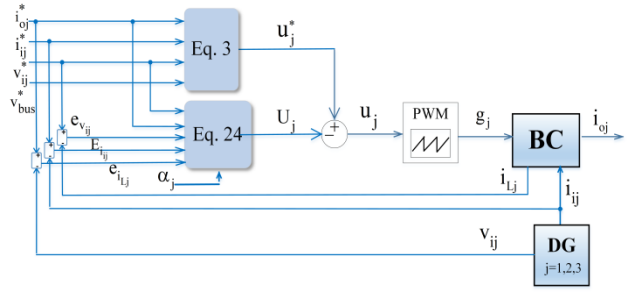

Figure 6. The detailed structure of the proposed BC controller.

4.2.2. Voltage stabilizing

The voltage control design is based on Equations (4), (18), and (25). According to Theorem 1, calculating U_n through Equation (25) will lead to system stability. Therefore, the controller calculates U_n at each step based on the state-feedback according to Figure 7. Since the switching function is placed in the energy equations equal to (18), by subtracting U_n from u_n^*, the modified switching functions are obtained dynamically and applied to the BBC.

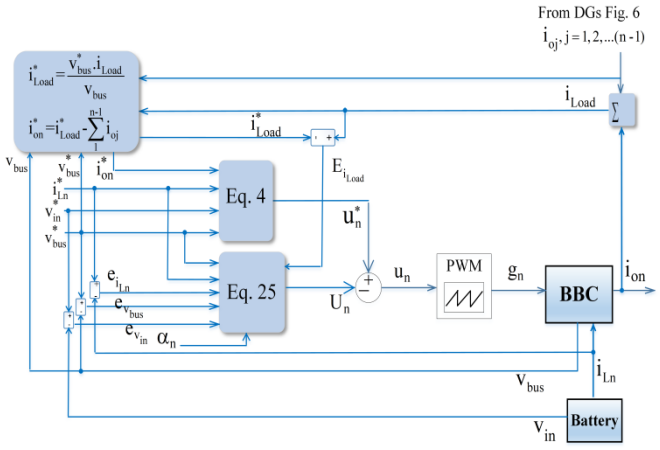

Figure 7. The detailed structure of the proposed BBC controller.

As can be seen in Equation (25), the effective variables and errors in the stabilization of the DC-bus voltage are involved in the calculation of the switching function. To adjust the DC-bus voltage to the desired value (v_{bus}^*), the deviation effects of the variables from their desired values are eliminated from the switching function by weighting α_n and consequently, according to Figure 7 the modified switching function is applied to the PWM. Based on the Equation (25), the factors such as the load variations, the inability of DG units to provide the needed power $(E_{i_{Load}})$, DC-bus voltage fluctuations $(e_{v_{bus}})$, and the deviations of the input voltage of the converter relative to its nominal value $(E_{v_{in}})$, affect the dynamical component of the switching function.

Based on Figure 7, to stabilize the DC-bus voltage and supply the load, the required load demand (i_{Load}^*) is subtracted from the total actual generated current of the DG units $(\sum_{1}^{n-1} i_{oj})$ and the result is considered as the desired reference current of the BESS unit (i_{on}^*). Obviously, when the total output power of the DG units exceeds the load demand, the (i_{on}) will be negative and the battery will be charged. Choosing the proper and accurate Lyapunov function has resulted in the participation of all effective errors on the DC-bus voltage stabilization in Equation (25). As can be seen in Figure 7, the BESS unit controller, in addition to stabilizing the fluctuations of the DC-bus voltage, compensates the needed current. Thus, in this scheme, the proper performance of the proposed BC controllers is its ability to reduce the contribution of the BESS unit to the transient and steady-state operation and consequently the proper performance of the BBC controller connected to the BESS unit, is its ability to inject needed currents, stabilize the DC-bus voltage through eliminating the fluctuations in transient and steady-state operation. As can be seen from Figures 6 and 7, the communication needs between the controllers are at their minimum level due to the independent operation of the BC controllers. Based on Figure 1, the only one-way communication is conducted via the BBC controller connected to the BESS.

5. SIMULATION AND RESULTS

In this section, to validate the performance of the proposed controller, a simulation has been performed in the MATLAB/SIMULINK® software. In this simulation, a stand-alone DC micro-grid consisting of two RERs, one fossil fuel energy resource, and one BESS that are a photovoltaic array, a wind-turbine unit, a gas-micro-turbine unit, and a lithium battery, respectively. The structure of the simulated micro-grid is shown in Figure 8. This micro-grid feeds a variable resistive load and the equations of $(v_{ij}, i_{ij}, j = 1,2,3,4)$ correspond to the [29, 35]. The DGs, BESS unit and the electrical load are connected to a common DC-bus. Further details about the parameters of the micro-grid have been listed in Table 1. To evaluate the performance of the controllers, several events are compiled in the form of two scenarios in sections 5.1 and 5.2 respectively. These considered events including the step changes in the reference values of the output currents (i_{oj}^*), the load changes, the simultaneous changes in generation level, the imbalance between generation and consumption, and the sudden disconnecting of a resource. As can be seen from the results, the proposed controller has a proper operation and is able to supply the load with desirable values of current and voltage, stability, and acceptable rapidity and accuracy. In Section 5.3, the performance of the proposed controller is investigated using multiple α_j. Finally, in section 5.4, to validate the proposed controller, its performance is compared with a conventional PI controller applied to the PWM.

Table 1. The details of the simulated DC micro-grid.

Parameter	Value	Parameter	Value
DC-bus voltage	950 (V)	Battery capacity	10 (Ah)
BC & BBC output capacitance	2.1 (mF)	Battery nominal voltage	1340 (V)
BC input capacitance	1 (mF)	BC & BBC inductance	5 (mH)
Switching frequency	5 (kHz)	BC & BBC input voltage	1400 (V)
Resistive load	19.95-31.35 (kW)	Number of DGs Number of BESS	3 1

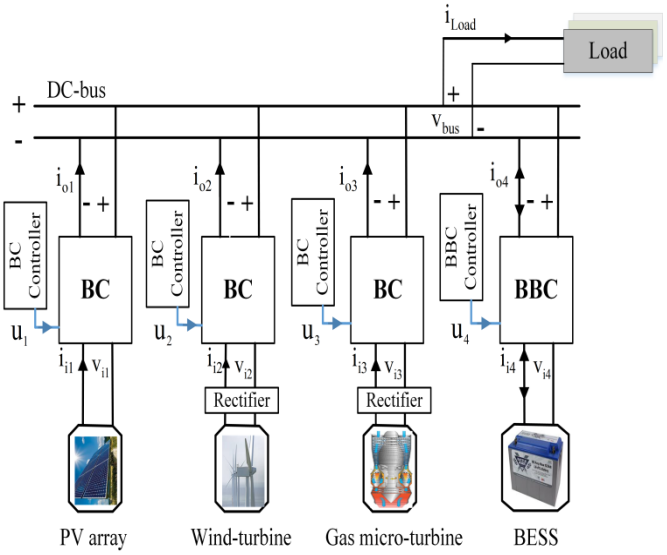

Figure 8. The structure of the simulated stand-alone DC micro-grid.

5.1. Scenario I: The changes in the load side

In this scenario, at first, the contribution rate of all DG units is assumed constant and the primary load demand is equal to 24(A). In two steps, the load increment at t=1 s and t=2 s, as well as in the next step, the load decrement at t=3 s are applied. These changes of load demand are respectively equal to +3(A), +6(A), and -12(A). The output current of each converter $(i_{oj,\,j=1,2,3,4})$, is shown in Figure 9. Moreover Figure 10 shows the total generated current, load demand (i_{Load}, i^{*}_{Load}), and the DC-bus voltage (v_{bus}). In Figure 9 the currents are displayed with more precise scale for greater clarity. Based on this figure, the load change has slight effects on the output currents of the BCs, with maximum oscillation range around 1.5 %. These oscillations are well removed. It means that the BC controllers have proper performance in the tracking of their set points $(i^{*}_{oj,\,j=1,2,3})$, because the BBC controller and BESS quickly compensate for the voltage drop caused by the increased load (Figure 10). Moreover, the BBC controller connected to the BESS unit performed well between t=1-3 s through regulating the current (i_{o4}) to meet the increment of the load requirement and in this way, the DC-bus voltage has been kept constant properly. In each event, new reference values are reflected along with the errors caused by the transient-states through Equations (24) and (25) in U_j. The new U_j is then deducted from u^{*}_j, thereby reducing the reflection of these fluctuations in the output current. The very slight saw-tooth fluctuations observed in the steady-state currents are related to the switching effect of the converters and are inevitable.

According to Figure 10, the DC-bus voltage has slight variations during the load changes, with quickly transient states. Moreover, to balance the needed and generated power, the BBC controller puts the BESS unit in the charge mode at t=3 s. After each event, the partial oscillations of the transient state in the output currents of the BCs are due to changes in the DC-bus voltage caused by sudden changes of the load. Changing the load causes a change in the equivalent impedance of the system. As can be seen in Figure 9, when the load increases (resistance decreases), the duration of the transient-state is longer than the load reduction state (increase in resistance). However, these fluctuations are dampened by a very slight range. Moreover, the BESS unit compensates for the DC-bus voltage with minimal fluctuations.

Theoretically, in this scenario, the effects of the DC-bus voltage errors are reflected by Equation (25) through considering $e_{v_{bus}}$ in the modified switching function of the BBC controller which results in the rapid elimination of fluctuations from the DC-bus voltage. Moreover, $\dot{W}(x)$ is calculated using equation (16) and shown in Figure 11. As can be seen in this figure, during Scenario I, $\dot{W}(x)$ is negative. Since $W_e(x) > 0$, based on (26), this result validates the stability of the system introduced by Theorem 1.

More details about the events and their results related to each scenario are listed in Table 2. In this table, i_{Load} is the steady-state current of the load, v_{bus} the steady-state voltage of the DC-bus that is equal to the load voltage. The error $e_{v_{bus}}$% is the steady-state error of the DC-bus voltage, expressed as a percentage.

5.2. Scenario II: The changes in the generation side

In this scenario, the load is assumed constant while the desired set points of the output currents $(i^{*}_{oj,\,j=1,2,3})$ are changed as modeling of changes in the generation level of the resources. The reference currents are respectively reduced equal to 5(A), 4(A), and 2(A) in three stages, between t=4-6 s. According to Figure 12, it is observed that the transient-states caused by this change, rapidly disappear in the output currents of each BCs. Also, the amplitude of the oscillations is negligible. Since the generated currents are less than the load demand, the BBC controller puts the BESS unit in the discharging mode through reversing the current (i_{on}). The BESS unit quickly discharges and prevents the DC-bus voltage from decreasing. Based on Figure 13 the proposed controller has acceptable performance in voltage stabilization. In this scenario, the desired reference currents $(i^{*}_{oj,\,j=1,2,3,4})$ and $(i^{*}_{ij,\,j=1,2,3,4})$ are changed.

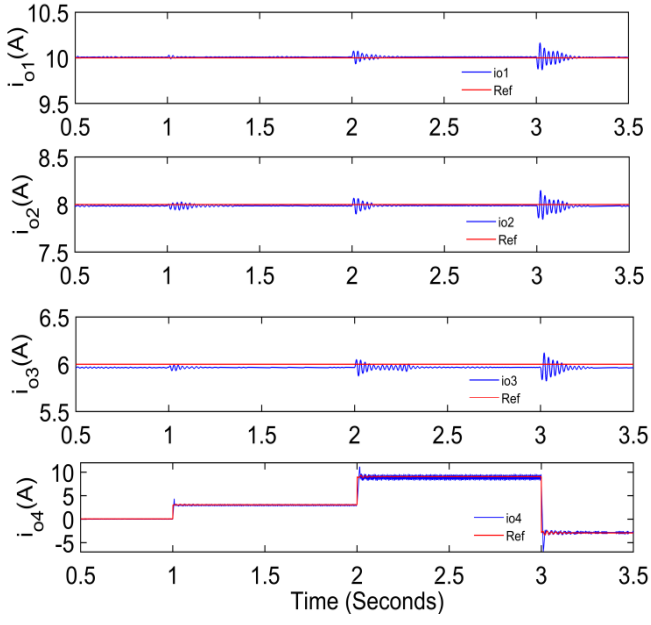

Figure 9. The output currents of DGs $(i_{oj,\,j=1,2,3})$ and BESS unit (i_{o4}) under load change during Scenario I.

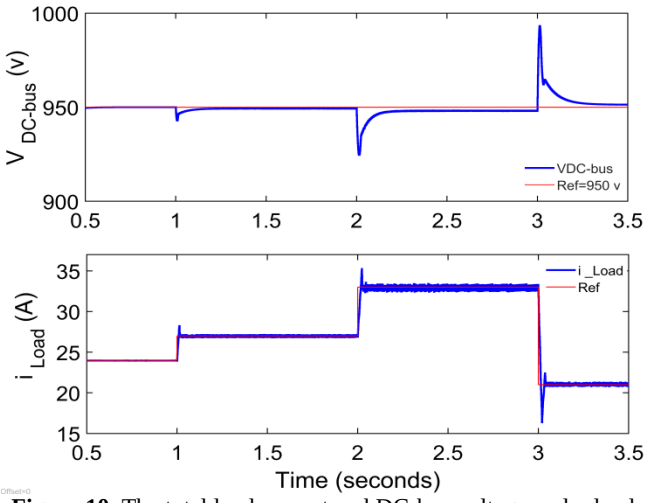

Figure 10. The total load current and DC-bus voltage under load change during Scenario I.

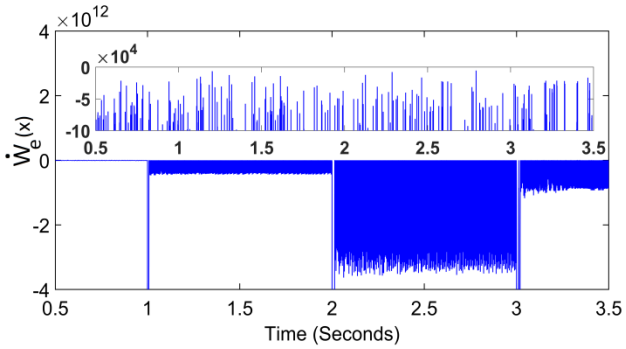

Figure 11. Calculating the derivative of energy function according to Equation (16) during Scenario I.

As mentioned in section 3, $(i^*_{oj} = i^*_{Lj,\, j=1,2,3})$ and $(i^*_{in} = i^*_{Ln})$. Therefore, based on Equations (24) and (25), these new reference values are included in the calculation along with their error values $(E_{i_{Load}}, E_{i_{ij}}, e_{i_{Lj}}, e_{i_{Ln}})$, and in this way, they are reflected in the modified switching functions (u_j). Consequently, in addition to generating new output currents (i_{oj}), the effects of their fluctuations are compensated properly. Moreover, in a harsh condition at t=7 s the desired output currents of DGs are increased simultaneously equal to 7(A) for each one, which is a serious stress for the system. As the output current exceeds the load demand, the BBC controller puts the BESS unit in the charging mode again. According to Figure 12, the transient-state caused by this change disappears rapidly in the output currents, and the amplitude of the oscillations is negligible. The BC controllers quickly attenuate the fluctuations caused by these changes by applying the error effects through Equation (24). Moreover, the output currents follow their set-points properly in the steady-state with acceptable accuracy. In addition, the BESS unit compensates the oscillations of the transient-state instantly. The DC-bus voltage is depicted in Figure 13. Based on this figure, in the steady-state, the BESS unit prevents the DC-bus voltage from increasing, and the proposed controller has proper performance against the changes of the generation set points. Based on section 4.2.2 i^*_{o4} is set equal to $i^*_{o4} = i^*_{Load} - \sum_{1}^{3} i_{oj}$. Hence, according to Figure 12, i^*_{o4} may be inherently oscillating. So, it does not interfere with stability. For instance, at t=7-8 s after a sudden step change in generation equal to +21(A), the fluctuation of i^*_{o4} are equal to the sum of the switching effects of the four converters and $(i_{o4} - i^*_{o4})$ is damping. The proposed controller is able to damp the oscillations well and ensure stability.

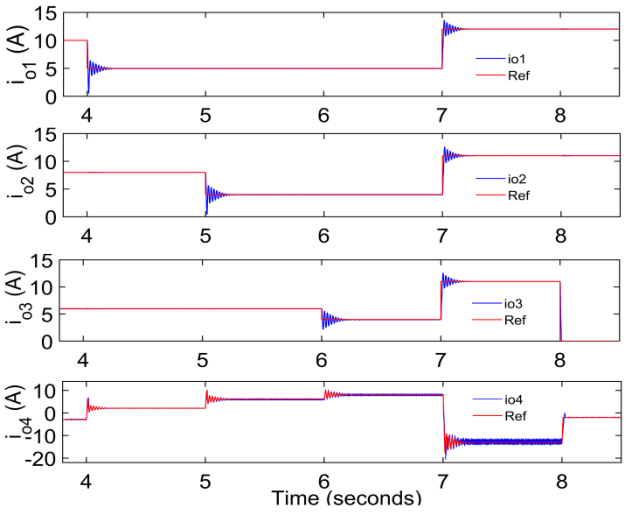

Figure 12. The output currents of DGs $(i_{oj,\, j=1,2,3})$ and BESS unit (i_{o4}) during Scenario II.

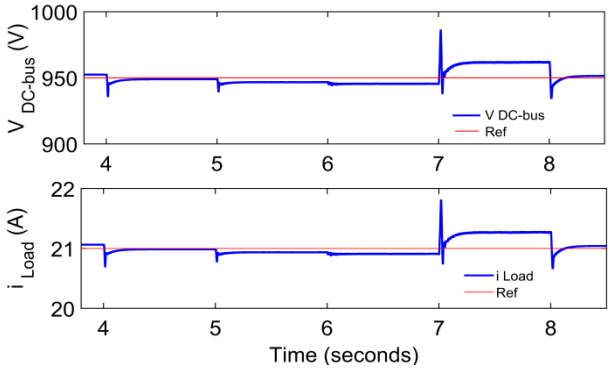

Figure 13. The total load current and DC-bus voltage during Scenario II.

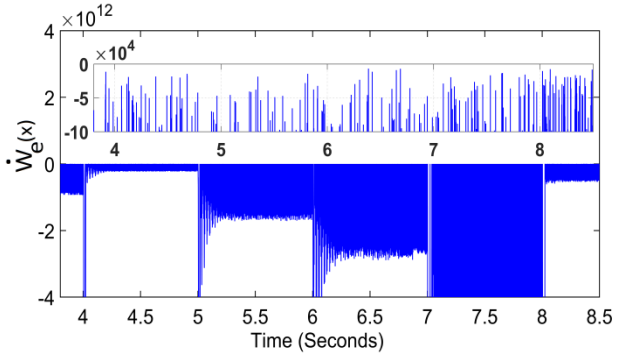

Figure 14. Calculating the derivative of energy function according to Equation (16) during Scenario II.

The steady-state error of the DC-bus voltage is equal to 1.26 %, which is still acceptable. In the following, at t=8 s, DG3 is abruptly disconnected from the micro-grid thus losing a significant portion of the generations, equal to 11(A). As a

result, based on Figure 13, the voltage drop occurs in DC-BUS. The BBC controller quickly alleviates this voltage drop through changing the contribution of BESS unit. As can be seen from Figure 12, DG1 and DG2 follow their set-points after a very slight and rapid transition. Moreover, $\dot{W}_e(x)$ is calculated and shown in Figure 14 during this scenario. As can be seen in this figure, during the events, $\dot{W}_e(x)$ is negative and based on (26), validates the stability of the system introduced by Theorem 1. Further details of the simulation results are given in Table 2.

Table 2. The summary of the events and their results.

	Time (s)	Events	i^*_{Load} (A)	i_{Load} (A)	v_{bus} (V)	$E^{(\%)}_{i_{Load}}$	$e^{(\%)}_{v_{bus}}$
Scenario I	t<1	Load=cte	24	23.95	950.01	-0.21	+0.001
	1	Load↑	27	26.95	948.80	-0.17	-0.120
	2	Load↑	33	32.90	946.60	-0.30	-0.350
	3	Load↓	21	21.15	952.50	+0.71	+0.260
Scenario II	4	DG1↓	21	20.96	948.88	-0.19	-0.120
	5	DG2↓	21	20.78	946.70	-1.05	-0.350
	6	DG3↓	21	20.70	945.50	-1.43	-0.470
	7	DG1,2,3↑	21	21.31	962.00	+1.47	+1.260
	8	DG3:off	21	21.08	951.75	+0.38	+0.180

5.3. The effects of the proposed controller on transient-state, accuracy, and stability

In this section, in order to investigate the effect of the proposed controller on the performance of DGs, the generated current of one of the DGs (i_{o1}) is simulated with different coefficients of the controller (α_1). According to Theorem 1, the system error for $\alpha_1 < 0$ will be dampened. Three allowed values are assigned to α_1. The considered events are according to Table 1 at t=3 s, 4 s. As can be seen in Figure 15, changing the α_1 leads to a change in the speed and accuracy of the controller. According to Equation (24), changing the α_1 changes the weight of the error term $(i^*_{Lj}e_{v_{ij}} - v^*_{ij}e_{i_{Lj}})^2$ on closed-loop. For this reason, $(\alpha_1 = -0.001)$ causes lower undershoot and higher steady-state error, $(\alpha_1 = -0.8)$ causes higher undershoot and higher steady-state accuracy. Also, $(\alpha_1 = -0.005)$ causes a moderate mode. This feature makes the controller flexible in various applications based on exploitation policy. It should be noted that theoretically, the curves related to $(\alpha_1 = -0.001)$ and $(\alpha_1 = -0.005)$ also move towards the reference with a very slight slope, in this case, a secondary controller can quickly reduce the steady-state error. However, it occurs much faster by applying $(\alpha_1 = -0.8)$, and if necessary, the proper filters can be used to compensate for the transient-state fluctuations. Moreover, as can be seen in Figure 16 and based on Equations (23) and (24), applying a positive coefficient $(\alpha_1 = 1)$ causes system instability. In this case, the values of U_1 will cause the $\dot{W}_e(x)$ to be positive and the errors will be incremental.

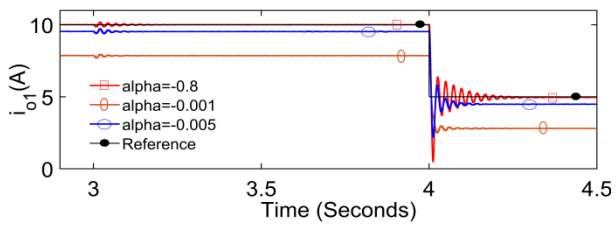

Figure 15. Comparing the generated current (i_{o1}) with various negative coefficients $(\alpha_1 = -0.001, -0.005, -0.8)$.

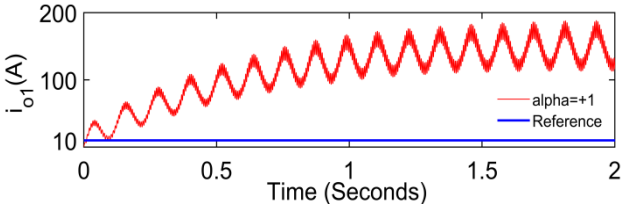

Figure 16. The generated current (i_{o1}) with positive coefficient $(\alpha_1 = +1)$.

5.4. Comparison of the proposed controller with conventional PI controller

In this section, the performance of the proposed controller is compared with the conventional PI controller [20, 21]. As mentioned, the application of linear controllers on non-linear systems is sensitive to changes in reference values [22]. In this comparison, the values of α_j have been set equal to 0.25 for all units. The PI controller issues the switching functions (u_j) by comparing (i_{oj}, i^*_{oj}). The PI controller is set so that both controllers perform the same function before changing the reference values $(i^*_{o1} = 2,\ i^*_{o2} = 8,\ i^*_{o3} = 6(A))$. Then, at t=1 s, i^*_{o1} changes equal to +13(A) and at t=2 s, i^*_{o2} and i^*_{o3} change respectively equal to -7(A) and +10(A). Figure 17 shows i_{oj} considering both control methods. Based on this figure, at t=1 s and t=2 s, a significant transient-states and steady-state fluctuations related to i_{o1} and i_{o3}, are observed in the performance of the PI controller compared to the proposed controller. Because in the PI controller, only the output current error is considered and u_j will fluctuate in proportion to current oscillation, which will cause more oscillation. However, in the proposed control method, the average of the switching function u^*_j is always constant and U_j dynamically corrects the switching functios $(u_j = u^*_j - U_j)$ based on Equations (24) and (25) and considering the errors of all state-variables. This feature reduces the amplitude and duration of transient-state oscillations. At t=2 s, after a sharp decrease, i_{o2} has been cut-off using the PI controller due to the presence of

a rectifier according to Figure 8 which prevents reverse current. However, this causes destructive tensions in the converter. Also, according to Figure 17, severe fluctuations of i_{oj} have led to significant battery participation using PI controller that will reduce battery life-span.

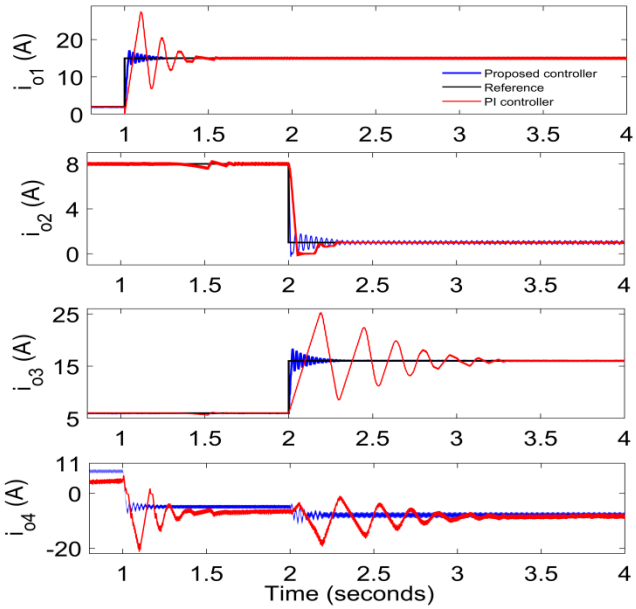

Figure 17. Comparison of the proposed controller with conventional PI control.

6. CONCLUSIONS

In this paper, a novel local controller for a multi-resource converter-based stand-alone DC micro-grid has been proposed based on DLM. A comprehensive dynamic micro-grid model associated with the converter-based ESS, RERs and gas-micro-turbine has been considered. In this proposed method, the steady-state and dynamic components of the switching functions have been separately investigated in the dynamic model to decrease the fluctuations due to the load alterations and performance of the DGs. Thereby, the controller ensures the fluctuation damping of the output and system stability. Besides, the proposed method ensures stable performance regardless of the dynamic equations of the resources and the number of DGs. Moreover, the independence of the DG controllers, simplicity, and easy execution are the other advantages of this method. The desired DC-bus voltage, accurate current generation, and fast response have been achieved by simulation in the MATLAB/SIMULINK® environment for various operating conditions. The simulation results show that the DGs are controlled individually with the negligible effects on each other. Moreover, the controllers exhibited good performance compared to conventional PI controllers in eliminating the oscillations caused by sudden changes in the generation, and are flexible in various applications based on exploitation policy. It can be predicted for example the combining an outer layer fuzzy or neural controller with the proposed method to adjust the alpha coefficients can be considered as future works.

7. ACKNOWLEDGEMENT

The authors acknowledge the support of Babol Noshirvani University of Technology through Grant program No. BNUT/925120010/2020.

REFERENCES

1. Rezagholizadeh, M., Aghaei, M. and Dehghan, O., "Foreign direct investment, stock market development, and renewable energy consumption: Case study of Iran", ***Journal of Renewable Energy and Environment (JREE)***, Vol. 7, No. 2, (2020), 8-18.
2. Carrasco, J.M., Franquelo, L., Bialasiewicz, J., Galvan, E., Portillo, R., Prats, M.M., Leon, J. and Moreno-Alfonso, N., "Power-electronic systems for the grid integration of renewable energy sources", ***Industrial Electronics, IEEE Transactions A: Survey***, Vol. 53, (2006), 1002-1016. (DOI: 10.1109/TIE.2006.878356).
3. Justo, J.J., Mwasilu, F., Lee, J. and Jung, J.W., "AC-micro-grids versus DC-micro-grids with distributed energy resources", ***Renewable and Sustainable Energy Reviews A: Review***, Vol. 24, (2013), 387-405. (DOI: 10.1016/j.rser.2013.03.067).
4. Elsayed, A.T., Mohamed, A.A. and Mohammed, O.A., "DC micro-grids and distribution systems", ***Electric Power Systems Research A: Overview***, Vol. 119, (2015), 407-417. (DOI: 10.1016/j.epsr. 2014.10.017).
5. Azizi, N. and Moradi CheshmehBeigi, H., "Reactive and active power control of grid WECS based on DFIG and energy storage system under both balanced and unbalanced grid conditions", ***Journal of Renewable Energy and Environment (JREE)***, Vol. 4, No. 4, (2017), 31-38.
6. Rahmani, M., Faghihi, F., Moradi CheshmehBeigi, H. and Hosseini, S., "Frequency control of islanded microgrids based on fuzzy cooperative and influence of STATCOM on frequency of microgrids", ***Journal of Renewable Energy and Environment (JREE)***, Vol. 5, No. 4, (2019), 27-33.
7. Joung, K.W., Kim, T. and Park, J.W., "Decoupled frequency and voltage control for stand-alone microgrid with high renewable penetration", ***IEEE Transactions on Industry Applications***, Vol. 55, No. 1, (2018), 122-133. (DOI: 10.1109/tia.2018.2866262).
8. Kim, J.Y., Jeon, J.H., Kim, S.K., Cho, C., Park, J.H., Kim, H.M. and Nam, K.Y., "Cooperative control strategy of energy storage system and micro sources for stabilizing the micro-grid during islanded operation", ***IEEE Transactions on Power Electronics***, Vol. 25, No. 12, (2010), 3037-3048. (DOI: 10.1109/TPEL.2010.2073488).
9. Dastgeer, F. and Gelani, H.E., "A comparative analysis of system efficiency for AC and DC residential power distribution paradigms", ***Energy and Buildings***, Vol. 138, (2017), 648-654. (DOI: 10.1016/j.enbuild.2016.12.077).
10. Xu, L. and Chen, D., "Control and operation of a DC micro-grid with variable generation and energy storage", ***IEEE Transactions on Power Delivery***, Vol. 26, No. 4, (2011), 2513-2522. (DOI: 10.1109/TPWRD.2011.2158456).
11. Fallah, S., Deo, R., Shojafar, M., Conti, M. and Shamshirband, S., "Computational intelligence approaches for energy load forecasting in smart energy management grids", ***State of the Art, Future Challenges, and Research Directions Energies***, Vol. 11, No. 3, (2018), 596. (DOI: 10.3390/en11030596).
12. Chen, D., Xu, L. and Yao, L., "DC voltage variation based autonomous control of DC micro-grids", ***IEEE Transactions on Power Delivery***, Vol. 28, No. 2, (2013), 637-648. (DOI: 10.1109/TPWRD. 2013.2241083).
13. Augustine, S., Mishra, M.K. and Lakshminarasamma, N., "Adaptive droop control strategy for load sharing and circulating current minimization in low-voltage stand-alone DC micro-grid", ***IEEE Transactions on Sustainable Energy***, Vol. 6, No. 1, (2015), 132-141. (DOI: 10.1109/TSTE.2014.2360628).
14. Dizqah, A.M., Maheri, A., Busawon, K. and Kamjoo, A., "A multivariable optimal energy management strategy for stand-alone dc micro-grids", ***IEEE Transactions on Power Systems***, Vol. 30, No. 5, (2015), 2278-2287. (DOI: 10.1109/TPWRS.2014.2360434).
15. Anand, S., Fernandes, B.G. and Guerrero, J.M., "Distributed control to ensure proportional load sharing and improve voltage regulation in low voltage DC micro-grids", ***Fuel***, Vol. 3, No. 4, (2013). (DOI: 10.1109/TPEL.2012.2215055).
16. Kordkheili, H., Banejad, M., Kalat, A., Pouresmaeil, E. and Catalão, J., "Direct-lyapunov-based control scheme for voltage regulation in a three-phase islanded microgrid with renewable energy sources", ***Energies***, Vol. 11, No. 5, (2018), 1161. (DOI: 10.3390/en11051161).
17. Tahim, A.P.N., Pagano, D.J., Lenz, E. and Stramosk, V., "Modeling and stability analysis of islanded DC microgrids under droop control", ***IEEE***

Transactions on Power Electronics, Vol. 30, No. 8, (2014), 4597-4607. (DOI: 10.1109/TPEL.2014.2360171).

18. Herrera, L., Zhang, W. and Wang, J., "Stability analysis and controller design of DC microgrids with constant power loads", ***IEEE Transactions on Smart Grid***, Vol. 8, No. 2, (2015), 881-888. (DOI: 10.1109/TSG.2015.2457909).
19. Liu, S., Zhu, W., Cheng, Y. and Xing, B., "Modeling and small-signal stability analysis of an islanded DC microgrid with dynamic loads", ***Proceedings of 15th International Conference on Environment and Electrical Engineering***, (2015), 866-871. (DOI: 10.1109/EEEIC. 2015.7165277).
20. Ghanbari, N., Bhattacharya, S. and Mobarrez, M., "Modeling and stability analysis of a dc microgrid employing distributed control algorithm", ***Proceedings of 9th IEEE International Symposium on Power Electronics for Distributed Generation Systems***, (2018), 1-7. (DOI: 10.1109/PEDG.2018.8447707).
21. Makrygiorgou, D. and Alexandridis, A., "Stability analysis of dc distribution systems with droop-based charge sharing on energy storage devices", ***Energies***, Vol. 10, No. 4, (2017), 433. (DOI: 10.3390/en10040433).
22. Perez, F. and Damm, G., DC microgrids, In Microgrids design and implementation, (2019), 472-473. (DOI: 10.1007/978-3-319-98687-6_16).
23. Fei, G.A.O., Ren, K.A.N.G., Jun, C.A.O. and Tao, Y.A.N.G., "Primary and secondary control in DC microgrids", ***Journal of Modern Power Systems and Clean Energy A: Review***, Vol. *7*, No. 2, (2019), 227-242. (DOI: 10.1007/s40565-018-0466-5).
24. Sitbon, M., Aharon, I., Averbukh, M., Baimel, D. and Sassonker, M., "Disturbance observer based robust voltage control of photovoltaic generator interfaced by current mode buck converter", ***Energy Conversion and Management***, Vol. 209, (2020). (DOI:10.1016/j.enconman.2020.112622).
25. Amiri, H., Markadeh, G.A., Dehkordi, N.M. and Blaabjerg, F., "Fully decentralized robust backstepping voltage control of photovoltaic systems for DC islanded microgrids based on disturbance observer method", ***ISA Transactions***, (2020). (DOI: 10.1016/j.isatra. 2020.02.006).

26 Kumar, J., Agarwal, A. and Agarwal, V., "A review on overall control of DC microgrids", ***Journal of Energy Storage***, Vol. 21, (2019), 113-138. (DOI: 10.1016/j.est.2018.11.013).

27. Mehdi, M., Jamali, S.Z., Khan, M.O., Baloch, S. and Kim, C.H., "Robust control of a DC microgrid under parametric uncertainty and disturbances", ***Electric Power Systems Research***, Vol. 179, (2020). (DOI: 10.1016/j.epsr.2019.106074).
28. Nahata, P., Soloperto, R., Tucci, M., Martinelli, A. and Ferrari-Trecate, G., "A passivity-based approach to voltage stabilization in DC microgrids with ZIP loads", ***Automatica***, Vol. 113, (2020). (DOI: 10.1016/j.automatica.2019.108770).
29. Tani, A., Camara, M.B. and Dakyo, B., "Energy management in the decentralized generation systems based on renewable energy-Ultracapacitors and battery to compensate the wind/load power fluctuations", ***IEEE Transactions on Industry Applications***, Vol. 51, No. 2, (2015), 1817-1827. (DOI: 10.1109/TIA.2014.2354737).
30. Kumar, M., Srivastava, S.C., Singh, S.N. and Ramamoorty, M., "Development of a new control strategy based on two revolving field theory for single-phase VCVSI integrated to DC micro-grid", ***International Journal of Electrical Power & Energy System***s, Vol. 98, (2018), 290-306. (DOI: 10.1016/j.ijepes.2017.11.042).
31. Camara, M.B., Dakyo, B. and Gualous, H., "Polynomial control method of DC/DC converters for DC-bus voltage and currents management-Battery and supercapacitors", ***IEEE Transactions on Power Electronics***, Vol. 27, No. 3, (2012), 1455-1467. (DOI: 10.1109/TPEL.2011.2164581).
32. Gavagsaz-Ghoachani, R., Phattanasak, M., Martin, J.P., Nahid-Mobarakeh, B., Pierfederici, S. and Riedinger, P., "Observer and lyapunov-based control for switching power converters with LC input filter", ***IEEE Transactions on Power Electronics***, Vol. 34, No, 7, (2019), 7053-7066. (DOI: 10.1109/tpel.2018.2877180).
33. Muhammad, H.R., Power electronics handbook, Prentice Hall, (2001), 64-66.
34. Slotine, J.J.E. and Li, W., Applied nonlinear control, Englewood Cliffs, NJ: Prentice Hall, (1991), 65-66.
35. Guda, S.R., Wang, C. and Nehrir, M.H., "Modeling of microturbine power generation systems", ***Electric Power Components and Systems***, Vol. 34, No. 9, (2006), 1027-1041. (DOI: 10.1080/15325000600596767).